

# Anthropogenic CO<sub>2</sub> penetration in the northern Red Sea and in the Gulf of Elat (Aqaba)

Red Sea  
Gulf of Elat (Aqaba)  
Anthropogenic carbon dioxide  
Mer Rouge  
Golfe d'Eilat (Aqaba)  
CO<sub>2</sub> anthropogénique

Boris S. KRUMGALZ<sup>a</sup>, Jonathan EREZ<sup>b</sup>, Chen-Tung A. CHEN<sup>c</sup>

<sup>a</sup> National Institute of Oceanography, Tel-Shikmona, P.O. Box 8030, Haifa 31080, Israël.

<sup>b</sup> Hebrew University of Jerusalem, Geology Department, Jerusalem, Israël.

<sup>c</sup> National Sun Yat-Sen University, Institute of Marine Geology, Kaohsiung, Taiwan 80424, Republic of China.

Received 10/7/89, in revised form 16/2/90, accepted 21/2/90.

## ABSTRACT

The penetration of anthropogenic carbon dioxide in the northern Red Sea and in the Gulf of Elat (Aqaba) was studied using data obtained during the *Tiran-02* cruise (February 1982). The results obtained demonstrated that the entire water column of the Gulf of Elat was saturated with an excess of anthropogenic CO<sub>2</sub>, indicating winter overturning. In the Red Sea, the upper 200 m are very young with a very uniform excess carbon dioxide signal close to zero ( $0 \pm 7 \mu\text{mol kg}^{-1}$ ). The  $\Delta\Sigma\text{CO}_2^0$  values (the signal of anthropogenic CO<sub>2</sub> penetration, after reaching maximum negative values *ca.*  $-28 \pm 5 \mu\text{mol kg}^{-1}$  at  $600 \pm 100$  m, increase and remain almost constant at *ca.*  $-15 \pm 6 \mu\text{mol kg}^{-1}$  from 800 to 1500 m. The increase of  $\Delta\Sigma\text{CO}_2^0$  values below  $600 \pm 100$  m in the northern Red Sea was explained by the influence of the overflow of younger waters from the Gulf of Elat over the sill in the Strait of Tiran and by the inflow of young waters from the Gulf of Suez. The tongue of these young waters spreads at a depth of about 800-1500 m from the Strait of Tiran southward. Relatively old waters, characterized by maximum negative  $\Delta\Sigma\text{CO}_2^0$  values at a depth of *ca.*  $600 \pm 100$  m, are sandwiched between younger waters.

Comparison of the obtained results with the existing data from other expeditions proves that the mechanism of deep water formation in the northern Red Sea is seasonally independent and did not change from the GEOSECS expedition of 1977.

*Oceanologica Acta*, 1990, 13, 3, 283-290.

## RÉSUMÉ

### Pénétration du CO<sub>2</sub> anthropogénique dans le nord de la Mer Rouge et le golfe d'Eilat (Aqaba)

La pénétration du CO<sub>2</sub> anthropogénique dans le nord de la Mer Rouge et dans le golfe d'Eilat (Aqaba) est étudiée à partir des données de la campagne *Tiran-02* (février 1982). Les résultats montrent que toute la colonne d'eau du golfe d'Eilat est saturée en CO<sub>2</sub> anthropogénique, par suite du renouvellement hivernal. Dans la Mer Rouge, les 200 premiers mètres sont très jeunes, l'excès de CO<sub>2</sub> étant uniforme et voisin de zéro ( $0 \pm 7 \mu\text{mol kg}^{-1}$ ). Les valeurs de  $\Delta\Sigma\text{CO}_2^0$  passent par un minimum négatif d'environ  $-28 \pm 5 \mu\text{mol kg}^{-1}$  à  $600 \pm 100$  m, puis se stabilisent à environ  $-15 \pm 6 \mu\text{mol kg}^{-1}$  de 800 à 1500 m. L'augmentation de  $\Delta\Sigma\text{CO}_2^0$  au-dessous de  $600 \pm 100$  m dans le nord de la Mer Rouge est due à l'apport des eaux plus jeunes du golfe d'Eilat qui franchissent le seuil du détroit de Tiran, et à l'apport d'eaux jeunes en provenance du Golfe de Suez. Ces eaux jeunes se répandent vers le Sud, au-delà du détroit, entre 800 et 1500 m de profondeur. Une couche d'eaux relativement vieilles, caractérisées par des valeurs négatives extrêmes de  $\Delta\Sigma\text{CO}_2^0$ , est observée à une profondeur de l'ordre de  $600 \pm 100$  m. Les résultats obtenus et les données d'autres campagnes montrent que, dans le nord de la Mer Rouge, le mécanisme de formation des eaux profondes ne dépend pas de la saison, et n'a pas varié depuis la campagne GEOSECS de 1972.

*Oceanologica Acta*, 1990, 13, 3, 283-290.

## INTRODUCTION

Since the beginning of the Industrial Revolution in the middle of the last century, the amount of carbon dioxide in the earth's atmosphere has drastically increased due to burning of fossil fuel and deforestation, especially during the last century. The partial carbon dioxide pressure in the atmosphere has increased from a pre-industrial value in the range of either 260-290 ppm (Dyrssen and Wedborg, 1982) or  $268 \pm 13 \mu\text{atm}$  (Poisson and Chen, 1987, who gave an extensive review of past atmospheric  $\text{CO}_2$  values) to the present value of approximately 335 ppm (Dyrssen and Wedborg, 1982). It has been estimated that by the year 2000 the  $\text{CO}_2$  level in the atmosphere will be doubled (Anderson and Malahoff, 1977). The ecological effects of this phenomenon can hardly be overestimated, but the greatest danger seems to be of global climatic changes. Mercer (1978), Stuiver (1978) and many others have predicted that an increase in the atmospheric  $\text{CO}_2$  level will lead to a warming of the globe ("greenhouse effect") which will cause the melting of polar ice (Kellogg, 1979; Thompson and Schneider, 1981; Bently, 1983; Revelle, 1983). This could raise the sea level by as much as several meters (Hoffman *et al.*, 1983) and lead to major catastrophes in coastal cities (Chen and Lin, 1987). Intensive studies of the various aspects of the global carbon system are thus a matter of urgency and are being conducted in many countries. One of the most probable ways of the neutralization of the  $\text{CO}_2$  increase in the atmosphere is its penetration to the deep oceans, accompanied by the dissolution of  $\text{CaCO}_3$ , resulting in the increase of total carbonate in the ocean waters. The deep oceans may thus be considered as a major sink for excess carbon dioxide (Moore, 1987). According to various estimations, the residence time of the deep water ranges from 700-1000 years (Southam and Peterson, 1985) to 1600 years (Broecker, 1974); therefore, the sunken  $\text{CO}_2$  is effectively removed from the atmosphere during this time interval. Evidence of anthropogenic  $\text{CO}_2$  penetration in the world ocean has been reported during the last decade by numerous scientists (Brewer, 1978; Broecker *et al.*, 1979; Chen and Millero, 1979; Jones and Levy, 1981; Broecker and Peng, 1982; Chen and Drake, 1986; *etc.*).

The northern Red Sea-Gulf of Elat system has no water input from the surrounding land. Changes in the carbonate chemistry parameters of this system are consequently controlled by carbon dioxide penetration from the atmosphere to the seawater, by chemical processes in the water column, and by the water body formation mechanism. The study of this limited area cannot solve quantitatively the problem of the global ocean's role in the regulation of atmospheric carbon dioxide content. However, the anthropogenic carbon dioxide excess signal will be computed for use as a geochemical tracer.

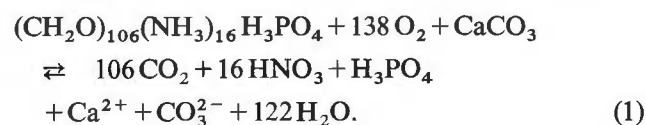
The Red Sea - Gulf of Elat system, part of the Syrian-African rift valley, is an embryonic ocean in the process of opening by sea floor spreading, in which the Gulf of Elat constitutes a deep and wide open fracture zone (Ben-Avraham *et al.*, 1979), separated from the Red

Sea by a shallow still (253 m, Anati, 1980) at the Strait of Tiran. The gulf itself reaches a maximum depth of ca. 1800 m. Its width is roughly 14-26 km and its length is ca. 180 km. The general winter circulation pattern in the Red Sea-Gulf of Elat has been studied during the past two decades and is described in Klinker *et al.* (1976) and Paldor and Anati (1979) for the Gulf of Elat, and in Morcos (1970), Manins (1973), Maillard (1974), Ross (1983), Poisson *et al.* (1984), Cember (1988) and Metzl *et al.* (1989) for the northern Red Sea.

The circulation pattern in the Gulf of Elat is driven mainly by thermohaline gradients and wind stress. Surface water of the northern Red Sea enters the Gulf of Elat through the Strait of Tiran and flows northward against the prevailing northern winds. These surface waters become cooler and more saline, hence denser. In the northern part of the Gulf of Elat, these dense waters sink and a return flow, developed above sill depth, forms part of the deep saline water in the northern Red Sea. Clearly the deep water in the northernmost Red Sea is formed by the overflow of cool and saline waters from both the gulfs of Elat and Suez. Therefore we can expect that various patterns of signal of anthropogenic  $\text{CO}_2$  penetration in these two water bodies (the Gulf of Elat and the Red Sea) will be observed.

## RESULTS AND DISCUSSION

A method for the calculation of the anthropogenic  $\text{CO}_2$  signal has been documented in Chen and Millero (1979) and Poisson and Chen (1987). Although the method is subject to large uncertainties (sometimes reaching  $\pm 20 \mu\text{mol kg}^{-1}$  according to Chen, 1982), the precision of the method is adequate to show the excess  $\text{CO}_2$  signal. Therefore the  $\text{CO}_2$  data can be very useful for tracing waters formed in the last 140 years (Chen, 1980). A portion of the surface seawater in contact with the air has a certain steady state carbon dioxide concentration. The amount of total dissolved carbon dioxide ( $\Sigma \text{CO}_2$ ) in this water is defined as  $\Sigma \text{CO}_2^0$ , which depends on the partial  $\text{CO}_2$  pressure in the air as well as the salinity and the temperature of the water. As the seawater portion sinks, the *in situ* decomposition of organic carbon and the dissolution of particulate  $\text{CaCO}_3$  add dissolved  $\text{CO}_2$  to this seawater portion. Consequently the measured  $\Sigma \text{CO}_2$  at each depth becomes larger than  $\Sigma \text{CO}_2^0$ . The values of  $\Sigma \text{CO}_2^0$  can be calculated from the measured  $\Sigma \text{CO}_2$  values for any particular depth by correcting them for carbon dioxide originating from organic carbon decomposition and  $\text{CaCO}_3$  dissolution. The chemically-added  $\text{CO}_2$  can in turn be calculated by the modified Redfield *et al.* (1963) model using the total titration alkalinity (TA) and the apparent oxygen utilization (AOU) data. The biological material decay model (Redfield *et al.*, 1963) with the addition of  $\text{CaCO}_3$  dissolution can be presented as:



According to equation 1, the combined effect of the dissolution of  $x$  moles of  $\text{CaCO}_3$  and decomposing  $y$  moles of organic matter in 1 kg of seawater on the changes of the concentrations of carbon, nitrogen, phosphorus, oxygen and TA can be represented as (Chen and Millero, 1978; Chen *et al.*, 1982a):

$$\Sigma \text{CO}_2 - \Sigma \text{CO}_2^0 = \Delta \Sigma \text{CO}_2 = x + 106y \quad (2)$$

$$\text{TA} - \text{TA}^0 = 2x - 17y \quad (3)$$

$$\text{AOU} = 138y \quad (4)$$

where  $\text{TA}^0$  is the titration alkalinity of the surface seawater portion, and AOU is the apparent oxygen utilization defined as the difference between the saturation values calculated for the potential temperature of the sample by the Weiss (1970) formula and the measured value at each depth:

$$\text{AOU} = \text{O}_{2(\text{sat})} - \text{O}_{2(\text{meas})} \quad (5)$$

Eliminating  $x$  and  $y$  from the equations 2-4 yields:

$$\Delta \Sigma \text{CO}_2 = 0.5[\text{TA} - \text{TA}^0] + 0.83 \text{AOU} \quad (6)$$

The right part of equation 6 represents the amount of total dissolved carbon dioxide originating from organic matter decomposition and  $\text{CaCO}_3$  dissolution. Thus, having the experimental values of total dissolved carbon dioxide ( $\Sigma \text{CO}_{2,\text{calc}}$ ) for each depth, we can calculate the total dissolved carbon dioxide content in this seawater portion at the time it was on the sea surface ( $\Sigma \text{CO}_{2,\text{old}}$ ):

$$\begin{aligned} \Sigma \text{CO}_{2,\text{old}} &= \Sigma \text{CO}_{2,\text{calc}} - \Delta \Sigma \text{CO}_2 \\ &= \Sigma \text{CO}_{2,\text{calc}} - 0.5[\text{TA} - \text{TA}^0] - 0.83 \text{AOU} \end{aligned} \quad (7)$$

Then the signal of anthropogenic  $\text{CO}_2$  penetration will be defined as follows:

$$\Delta \Sigma \text{CO}_2^0 = \Sigma \text{CO}_{2,\text{old}} - \Sigma \text{CO}_{2,\text{present}} \quad (8)$$

where  $\Sigma \text{CO}_{2,\text{old}}$  and  $\Sigma \text{CO}_{2,\text{present}}$  are the total dissolved carbon dioxide values for water formed some time ago and for water formed between 1981 and 1982, respectively. Thus, the values  $\Sigma \text{CO}_{2,\text{present}}$  are total dissolved carbon dioxide content for surface sea water at the sampling time.

The above scheme is based on the Redfield stoichiometry  $\text{C:N:P:O}_2 = 106:16:1:(-138)$  for organic matter suggested by Redfield *et al.* (1963) for the western Atlantic waters, and has been shown to be correct also in some other locations of the world ocean (*e.g.* Kumar, 1985). However, during recent years some data (*e.g.* Anderson and Dyrssen, 1981; Broecker and Peng, 1982; Takahashi *et al.*, 1985; Naqvi *et al.*, 1986; Pappaud and Poisson, 1986; Minster and Boulahdid, 1987; Peng and Broecker, 1987; Boulahdid and Minster, 1989) demonstrated that coefficients characterizing the ratio  $\text{C:N:P:O}_2$  sometimes differ from those suggested by equation (1). The variations in the  $\text{C:N:P:O}_2$  ratios reported for world ocean waters resulted in the variability of the coefficient connected to AOU in equations (6) and (7) (RKR factor) from 0.75 (Kroopnick, 1985) to 0.865 (Naqvi *et al.*, 1986). The item  $\text{RKR} \cdot \text{AOU}$  in equation (7) is a minor item, compared to the others,

and the use of one particular RKR value instead of another can result in only a minor bias in the calculated  $\Delta \Sigma \text{CO}_2^0$  values. Therefore the variation of the RKR factor, even between its extreme values, causes no appreciable changes in the conclusions.

The limitations of the  $\Delta \Sigma \text{CO}_2^0$  calculation method have been described in detail elsewhere (Chen and Millero, 1979; Chen and Pytkowicz, 1979; Chen *et al.*, 1982b; Shiller, 1981; Chen, 1982). Summarizing equations (7)-(8) gave results with a precision ranging from  $\pm 5$  to  $\pm 20 \mu\text{mol kg}^{-1}$  for various data sets, as stated by Chen (1982). Taking into account the experimental precision of our data (discussed below) and the scatter of the data, the uncertainties of the  $\Delta \Sigma \text{CO}_2^0$  values are actually as good as *ca.*  $\pm 10 \mu\text{mol kg}^{-1}$  for all the Tiran-02 cruise stations.

The calculations of the signal of anthropogenic  $\text{CO}_2$  penetration in the Red Sea and in the Gulf Elat were carried out using pH, total titration alkalinity (TA) and dissolved oxygen content, measured on board R/V *Shikmona* during the Tiran-02 cruise in February 1982. The whole track of the cruise is presented in Figure 1 with station description in Table 1. The experimental

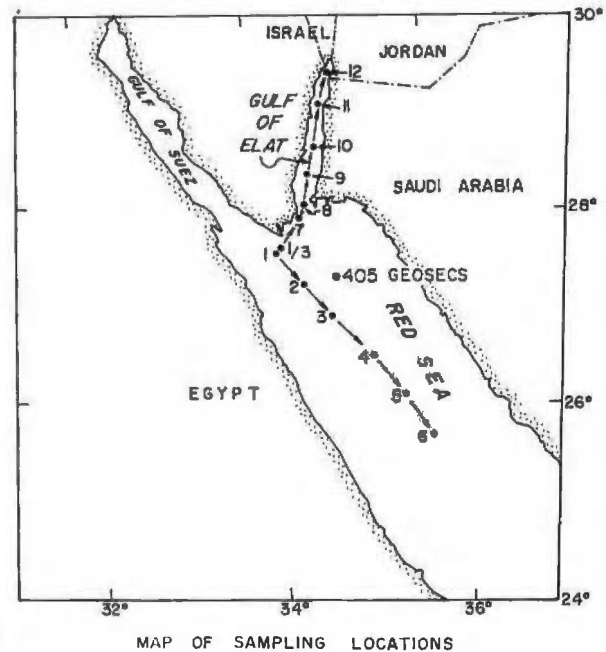


Figure 1  
Map of sampling locations for the Tiran-02 cruise.

Table 1  
Station description.

| Stn No. | Sampling date | Sampling time (local) | Station position |
|---------|---------------|-----------------------|------------------|
| 1       | 1 Feb. 82     | 13 <sup>00</sup>      | 27°33'N, 34°14'E |
| 2       | 1 Feb. 82     | 20 <sup>30</sup>      | 27°12'N, 34°32'E |
| 3       | 2 Feb. 82     | 06 <sup>10</sup>      | 26°54'N, 34°46'E |
| 4       | 2 Feb. 82     | 15 <sup>35</sup>      | 26°31'N, 35°09'E |
| 5       | 3 Feb. 82     | 01 <sup>00</sup>      | 26°05'N, 35°25'E |
| 6       | 3 Feb. 82     | 10 <sup>45</sup>      | 25°43'N, 35°46'E |
| 1/3(*)  | 5 Feb. 82     | 10 <sup>30</sup>      | 27°35'N, 34°13'E |
| 7       | 5 Feb. 82     | 19 <sup>20</sup>      | 27°55'N, 34°26'E |
| 8       | 6 Feb. 82     | 01 <sup>30</sup>      | 27°59'N, 34°27'E |
| 9       | 6 Feb. 82     | 07 <sup>35</sup>      | 28°18'N, 34°31'E |
| 10      | 6 Feb. 82     | 17 <sup>35</sup>      | 28°40'N, 34°37'E |
| 11      | 6 Feb. 82     | 23 <sup>15</sup>      | 29°05'N, 34°43'E |
| 12      | 7 Feb. 82     | 07 <sup>15</sup>      | 29°26'N, 34°53'E |

(\*) Sampling was conducted after a strong storm.

Table 2

Hydrographic data and carbonate chemistry parameters for the Tiran-02 cruise in the Gulf of Elat and the northern Red Sea in 1982.

| Depth (m) | pH <sub>in situ</sub> | TA, (meq kg <sup>-1</sup> ) | ΣCO <sub>2,calc.</sub> (mmol kg <sup>-1</sup> ) | AOU, (μmol kg <sup>-1</sup> ) |  |        |       |       |       |       |
|-----------|-----------------------|-----------------------------|---|-------------------------------|--|--------|-------|-------|-------|-------|
|           |                       |                             |   |                               |  | 3.2    | —     | 2.506 | 2.052 | -2.0  |
|           |                       |                             |   |                               |  | 3.2    | —     | 2.506 | 2.052 | 3.8   |
|           |                       |                             |   |                               |  | 3.2    | —     | 2.506 | 2.052 | 2.8   |
|           |                       |                             |   |                               |  | 204.9  | —     | 2.503 | 2.073 | 19.7  |
|           |                       |                             |   |                               |  | 204.9  | —     | 2.503 | 2.073 | 21.7  |
|           |                       |                             |   |                               |  | 407.1  | —     | 2.492 | 2.106 | —     |
|           |                       |                             |   |                               |  | 407.1  | —     | 2.492 | 2.106 | —     |
|           |                       |                             |   |                               |  | 609.0  | —     | 2.478 | 2.156 | 125.8 |
|           |                       |                             |   |                               |  | 801.6  | —     | 2.478 | 2.111 | 126.7 |
|           |                       |                             |   |                               |  | 1077.5 | —     | 2.497 | 2.140 | —     |
|           |                       |                             |   |                               |  | 1077.5 | —     | 2.496 | 2.139 | —     |
|           |                       |                             |   |                               |  | 2.9    | 8.295 | 2.503 | 2.087 | 4.7   |
|           |                       |                             |   |                               |  | 75.1   | 8.295 | 2.516 | 2.097 | 5.5   |
|           |                       |                             |   |                               |  | 148.3  | 8.291 | 2.507 | 2.090 | 6.4   |
|           |                       |                             |   |                               |  | 148.3  | 8.295 | 2.507 | 2.087 | 5.5   |
|           |                       |                             |   |                               |  | 198.7  | 8.264 | 2.523 | 2.125 | 23.9  |
|           |                       |                             |   |                               |  | 248.0  | 8.245 | 2.511 | 2.128 | 37.4  |
|           |                       |                             |   |                               |  | 298.4  | 8.250 | 2.508 | 2.120 | —     |
|           |                       |                             |   |                               |  | 496.8  | 8.195 | 2.508 | 2.154 | —     |
|           |                       |                             |   |                               |  | 694.1  | 8.085 | 2.505 | 2.218 | 145.2 |
|           |                       |                             |   |                               |  | 891.9  | 8.126 | 2.478 | 2.163 | 110.2 |
|           |                       |                             |   |                               |  | 1139.6 | 8.137 | 2.493 | 2.166 | 97.6  |
|           |                       |                             |   |                               |  | 3.4    | 8.322 | 2.524 | 2.086 | 4.9   |
|           |                       |                             |   |                               |  | 149.5  | 8.309 | 2.517 | 2.090 | 8.7   |
|           |                       |                             |   |                               |  | 368.9  | 8.284 | 2.510 | 2.099 | 19.4  |
|           |                       |                             |   |                               |  | 2.9    | 8.296 | —     | —     | 6.0   |
|           |                       |                             |   |                               |  | 48.9   | 8.295 | —     | —     | 6.8   |
|           |                       |                             |   |                               |  | 89.4   | 8.285 | —     | —     | 10.4  |
|           |                       |                             |   |                               |  | 118.0  | 8.284 | —     | —     | 2.7   |
|           |                       |                             |   |                               |  | 159.5  | 8.282 | —     | —     | 10.8  |
|           |                       |                             |   |                               |  | 249.2  | 8.277 | —     | —     | 12.8  |
|           |                       |                             |   |                               |  | 299.5  | 8.264 | —     | —     | 17.4  |
|           |                       |                             |   |                               |  | 399.5  | 8.244 | —     | —     | 35.2  |
|           |                       |                             |   |                               |  | 497.9  | 8.234 | —     | —     | 41.2  |
|           |                       |                             |   |                               |  | 595.7  | 8.227 | —     | —     | 44.3  |
|           |                       |                             |   |                               |  | 743.2  | 8.222 | —     | —     | 45.3  |
|           |                       |                             |   |                               |  | 950.5  | 8.212 | —     | —     | 47.1  |
|           |                       |                             |   |                               |  | 3.6    | 8.271 | 2.512 | 2.118 | 4.8   |
|           |                       |                             |   |                               |  | 99.8   | 8.267 | 2.510 | 2.117 | 5.7   |
|           |                       |                             |   |                               |  | 200.1  | 8.261 | 2.514 | 2.122 | 5.7   |
|           |                       |                             |   |                               |  | 299.1  | 8.237 | 2.506 | 2.131 | 22.9  |
|           |                       |                             |   |                               |  | 399.7  | 8.218 | 2.512 | 2.149 | 36.5  |
|           |                       |                             |   |                               |  | 791.2  | 8.190 | —     | —     | 45.6  |
|           |                       |                             |   |                               |  | 990.6  | 8.182 | 2.502 | 2.152 | 43.6  |
|           |                       |                             |   |                               |  | 1138.5 | 8.177 | 2.505 | 2.153 | 45.4  |
|           |                       |                             |   |                               |  | 1285.7 | 8.174 | 2.500 | 2.149 | 44.4  |
|           |                       |                             |   |                               |  | 1384.8 | 8.178 | 2.497 | 2.141 | 45.3  |
|           |                       |                             |   |                               |  | 1505.5 | 8.161 | 2.498 | 2.151 | 46.2  |
|           |                       |                             |   |                               |  | 3.4    | 8.281 | —     | —     | 6.0   |
|           |                       |                             |   |                               |  | 59.8   | 8.283 | —     | —     | 5.8   |
|           |                       |                             |   |                               |  | 118.7  | 8.279 | —     | —     | 5.8   |
|           |                       |                             |   |                               |  | 301.6  | 8.264 | —     | —     | 12.1  |
|           |                       |                             |   |                               |  | 337.0  | 8.248 | —     | —     | 26.9  |
|           |                       |                             |   |                               |  | 380.7  | 8.231 | —     | —     | 40.3  |
|           |                       |                             |   |                               |  | 447.5  | 8.223 | —     | —     | 42.3  |
|           |                       |                             |   |                               |  | 498.1  | 8.224 | —     | —     | 43.3  |
|           |                       |                             |   |                               |  | 595.6  | 8.213 | —     | —     | 44.3  |
|           |                       |                             |   |                               |  | 689.4  | 8.209 | —     | —     | 46.3  |
|           |                       |                             |   |                               |  | 790.1  | 8.201 | —     | —     | 48.2  |
|           |                       |                             |   |                               |  | 2.2    | 8.278 | 2.510 | 2.112 | 5.2   |
|           |                       |                             |   |                               |  | 98.9   | 8.281 | 2.511 | 2.108 | 6.1   |
|           |                       |                             |   |                               |  | 198.2  | 8.278 | 2.507 | 2.105 | 6.0   |
|           |                       |                             |   |                               |  | 296.4  | 8.274 | 2.506 | 2.104 | 4.9   |
|           |                       |                             |   |                               |  | 347.5  | 8.248 | 2.508 | 2.122 | 21.1  |
|           |                       |                             |   |                               |  | 397.1  | 8.225 | 2.506 | 2.139 | 40.5  |
|           |                       |                             |   |                               |  | 446.0  | 8.217 | 2.507 | 2.145 | 41.7  |
|           |                       |                             |   |                               |  | 595.1  | 8.185 | 2.500 | 2.156 | 45.7  |
|           |                       |                             |   |                               |  | 694.3  | 8.203 | 2.506 | 2.148 | 46.6  |
|           |                       |                             |   |                               |  | 807.0  | 8.200 | 2.494 | 2.137 | 48.5  |
|           |                       |                             |   |                               |  | 3.0    | 8.271 | 2.496 | 2.092 | 3.8   |
|           |                       |                             |   |                               |  | 58.8   | 8.264 | 2.507 | 2.109 | 1.9   |
|           |                       |                             |   |                               |  | 178.1  | 8.205 | 2.495 | 2.144 | 53.6  |
|           |                       |                             |   |                               |  | 239.1  | 8.149 | —     | —     | 90.0  |
|           |                       |                             |   |                               |  | 298.5  | 8.114 | —     | —     | 117.2 |
|           |                       |                             |   |                               |  | 399.6  | 8.066 | 2.484 | 2.215 | 152.2 |
|           |                       |                             |   |                               |  | 496.5  | 8.059 | 2.477 | 2.210 | 143.1 |
|           |                       |                             |   |                               |  | 594.8  | 8.065 | 2.480 | 2.209 | 145.3 |
|           |                       |                             |   |                               |  | 794.4  | 8.084 | 2.474 | 2.188 | 130.7 |
|           |                       |                             |   |                               |  | 1090.0 | 8.103 | 2.476 | 2.173 | 107.3 |
|           |                       |                             |   |                               |  | 1239.6 | 8.107 | 2.477 | 2.167 | 101.4 |

results and the calculated total dissolved carbon dioxide are summarized in Table 2. The pH values presented in the table were calculated for *in situ* conditions according to Millero (1979).

Total alkalinity measurements were carried out by the method developed by Edmond (1970). The end-point

of titration was determined by an automatic digital titration system (Radiometer DTS-833) using a glass electrode (G2040C) and a calomel electrode (K4040). The total alkalinities in volumetric scale were converted to weight units using the seawater densities calculated by the one atmosphere International Equation of State

of Seawater 1980 (UNESCO, 1981). The precision of the total alkalinity determination was *ca.* 0.003 meqv  $\text{kg}^{-1}$ . pH measurements of seawater samples were carried out at 25°C with a precision of  $\pm 0.002$  pH in the water as soon as the samples were taken from the Niskin bottles, immediately after sampling for oxygen, in special vessels similar to those described in the UNESCO report (1983). A combined glass electrode (GK2401C) with a Radiometer pH meter (PHM64) were used for pH measurements. Oxygen analysis was conducted using the modified Winkler method (Strickland and Parsons, 1972) with a precision of  $\pm 0.5\%$  (one standard deviation). Details of the experimental part and calculations of the carbonate chemistry parameters have been reported earlier (Millero, 1979; Millero *et al.*, 1979; Krumgalz and Erez, 1984). All these parameters were calculated under *in situ* conditions, taking into account the temperature, pressure and salinity corrections. The apparent dissociation constants of carbonic and boric acids, valid for the high salinities encountered in the Red Sea, were taken from Mehrbach *et al.* (1973) and from Takahashi *et al.* (1970), respectively.

The  $\text{TA}^0$ ,  $\Delta\Sigma\text{CO}_2^0$  and other chemical properties, except AOU, have been normalized on a constant 35 salinity basis (to take account either evaporation or precipitation effects) as:

$$(\text{Property})_{\text{norm}} = (\text{Property})_{\text{meas}} \times 35.000/S_{\text{meas}} \quad (9)$$

where subscripts "norm" and "meas" relate to the normalized and measured properties, respectively.

Chen and Pytkowicz (1979) and Kroopnick (1985), using the GEOSECS expedition data for world oceanic waters, reported that  $\text{TA}^0$  and  $\Sigma\text{CO}_2^0$  showed linear temperature dependence in the natural temperature interval. As may be seen from Figure 2, based on our data for the surface waters of the northern Red

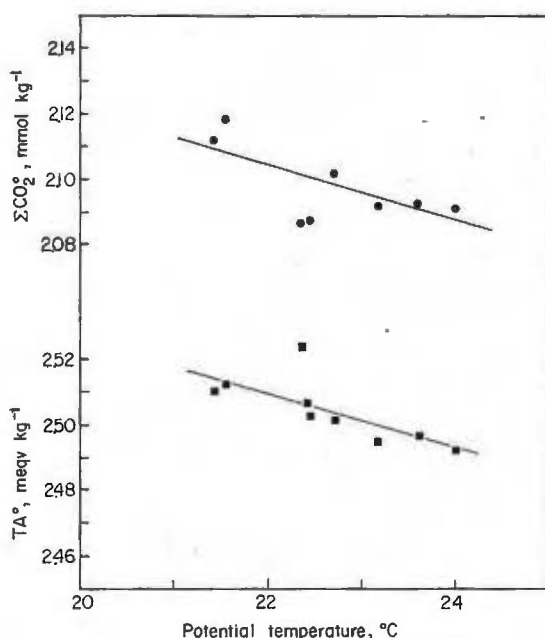


Figure 2  
Surface  $\Sigma\text{CO}_2^0$  and  $\text{TA}^0$  values normalized to 35 salinity at various potential temperatures.

Sea and the Gulf of Elat, such a relationship exists also in the area under study. The following equations represent the best fit of the *Tiran-02* cruise surface  $\text{TA}^0$  and  $\Sigma\text{CO}_2^0$  values:

$$\text{TA}^0 (\mu\text{eq kg}^{-1}) = 2698 - 8.5 \times \Theta (\pm 7) \quad (10)$$

$$\begin{aligned} \Sigma\text{CO}_2^0, \text{present} (\mu\text{mol kg}^{-1}) & \quad (11) \\ & = 2297 - 8.8 \times \Theta (\pm 9) \end{aligned}$$

where  $\Theta$  is the potential temperature, and the numbers in parenthesis are one standard deviation of the least squares fits. However, since temperature in the studied area changed in a very narrow range, we feel that the temperature normalization in this study can introduce only a negligible effect in the calculations and may therefore be omitted.

The calculated excess carbon dioxide signals ( $\Delta\Sigma\text{CO}_2^0$ ) based on *Tiran-02* cruise data (Krumgalz and Erez, 1984) for the Gulf of Elat and the northern Red Sea are presented in Figure 3. The  $\Delta\Sigma\text{CO}_2^0$  values are close

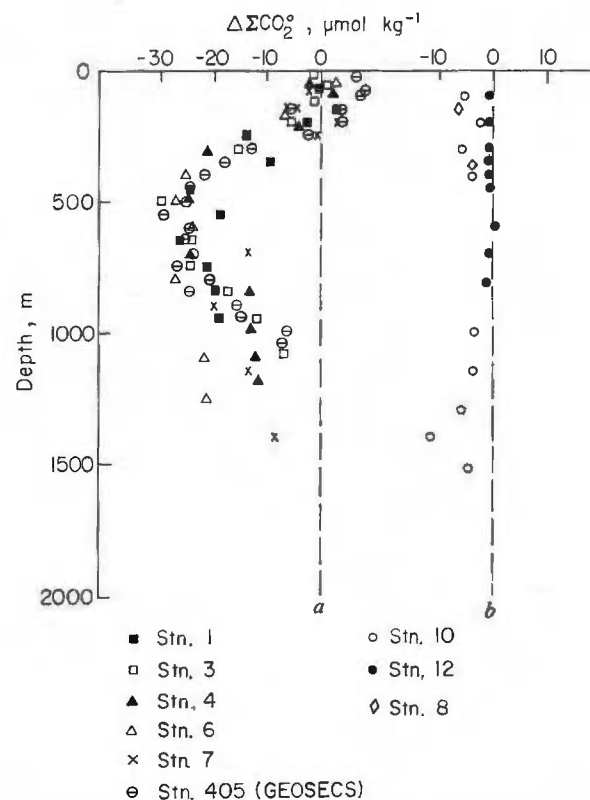


Figure 3  
Depth profiles of  $\Delta\Sigma\text{CO}_2^0$  for the Red Sea (a) and for the Gulf of Elat (b). The  $\Delta\Sigma\text{CO}_2^0$  values for station 405 (GEOSECS) were calculated from Weiss *et al.* (1983).

to zero for surface waters and for the mixed layer and become negative for deeper and older waters, because at the time when these waters were formed, their performed  $\Sigma\text{CO}_2^0, \text{old}$  values were lower than the present-day  $\Sigma\text{CO}_2^0, \text{present}$  values. In the northern Gulf of Elat (station 12), the entire water column seems to be saturated with excess anthropogenic  $\text{CO}_2$ , indicating winter overturning of the water column. However, in the central part of the Gulf of Elat (station 10), and even in

the vicinity of the Strait of Tiran (station 8), old waters (negative values of  $\Delta\Sigma\text{CO}_2^0$ ) can be observed at all depths. The results obtained for station 8, situated in the Strait of Tiran, are in good agreement with a well-developed two-layered gravitational convection circulation between the Red Sea and the Gulf of Elat (Murray *et al.*, 1984). The values of  $\Delta\Sigma\text{CO}_2^0$  for the northern Red Sea decrease from about 3 to  $-30\ \mu\text{mol kg}^{-1}$  (with uncertainties  $\pm 10\ \mu\text{mol kg}^{-1}$ ) from surface to the maximum studied depth *ca.* 1500 m, close to the sea floor. At depths of  $600\pm 100$  m, the  $\Delta\Sigma\text{CO}_2^0$  reaches a maximum negative value, showing the strong excess  $\text{CO}_2$  penetration in the Red Sea. These results, namely the general pattern of excess  $\text{CO}_2$  penetration in the Red Sea, are in very good agreement with those obtained by Papaud and Poisson (1986) in the Red Sea in summer 1982.

We could expect the anthropogenic  $\text{CO}_2$  tracer to have a distribution pattern similar to nuclear bomb tracers. In fact, the depth distribution pattern of the  $\Delta\Sigma\text{CO}_2^0$  signal for the northern Red Sea (Fig. 3) is similar to the tritium and  $\Delta^{14}\text{C}$  vertical profiles from GEOSECS Red Sea stations (Cember, 1988), and to the helium-3 data of Andrie and Merlivat (1989) for the *Merou* cruise (July 1982) in the Red Sea. After reaching maximum negative values,  $-28\pm 5\ \mu\text{mol kg}^{-1}$ , the  $\Delta\Sigma\text{CO}_2^0$  values increase and remain almost constant (in the uncertainty range), *ca.*  $-15\pm 6\ \mu\text{mol kg}^{-1}$ , from 800 to 1500 m, the lowest sampling depth close to the sea floor. The increase of  $\Delta\Sigma\text{CO}_2^0$  values below  $600\pm 100$  m can be explained by the outflow of younger waters from the Gulf of Elat (Cember, 1988) over the sill at the Straits of Tiran and from the Gulf of Suez (Morcos, 1970). A cross-section of the anthropogenic  $\text{CO}_2$  signal in the Gulf of Elat and in the northern Red Sea (Fig. 4) demonstrates very clearly the influence of the overflow of young waters from the Gulf of Elat over the sill at the Strait of Tiran and the inflow of young waters from the Gulf of Suez in the deepening of old waters at stations 1 and 7, closest to the Gulf of Suez and Strait of Tiran, respectively. The tongue of these young waters from the gulfs of Suez and Elat spreads at a depth of about 800-1500 m from the Strait of Tiran to the south. Relatively old waters,

characterized by maximum negative  $\Delta\Sigma\text{CO}_2^0$  values at a depth of *ca.*  $600\pm 100$  m, are sandwiched between younger waters.

Maximum of the anthropogenic  $\text{CO}_2$  signal found around 600 m is also related to the extremes of other properties such as nutrients (silicate, nitrate, phosphate),  $\Delta^{14}\text{C}$ , helium, tritium and oxygen (Weiss *et al.*, 1983; Krumgalz and Erez, 1984; Papaud and Poisson, 1986; Cember, 1988) at approximately the same depth. The specific features of this water layer at about 600 m depth is conditioned by three processes acting simultaneously in this area:

- intensive penetration of various geochemical tracers to depth;
- the intermediate return flow of seawater from the south in accordance with the circulation scheme presented by Manins (1973), Cember (1988) and Metz *et al.* (1989).
- the outflow of younger waters from the Gulfs of Elat and Suez.

Thus, the intermediate return flow leads to helium maximum owing to helium enrichment from the south, while the nutrient maximum and oxygen minimum are the results of the decline of the ventilation of this water layer. The simultaneous actions of the three above-mentioned processes are also responsible for the maximum of the anthropogenic  $\text{CO}_2$  signal at about 600 m. Just four years before the *Tiran-02* cruise, a GEOSECS expedition took place in the Mediterranean Sea and the Indian Ocean. One of the cruise stations (station 405) was situated not far from our station 3 in the Red Sea (see Fig. 1). Since station 405 (GEOSECS) was sampled in December 1977, it can be considered that this was during the same winter season as the *Tiran-02* cruise. Therefore, a comparison of the results obtained for these stations during various cruises would be of great interest, especially concerning any changes (if any) which may have occurred between 1977 and 1982. The  $\Delta\Sigma\text{CO}_2^0$  values for station 405 (GEOSECS) have been calculated by us from the GEOSECS cruise data (Weiss *et al.*, 1983) and plotted together with the *Tiran-02* data in Figure 3. We used for calculation purposes  $\Sigma\text{CO}_2$  values measured exper-

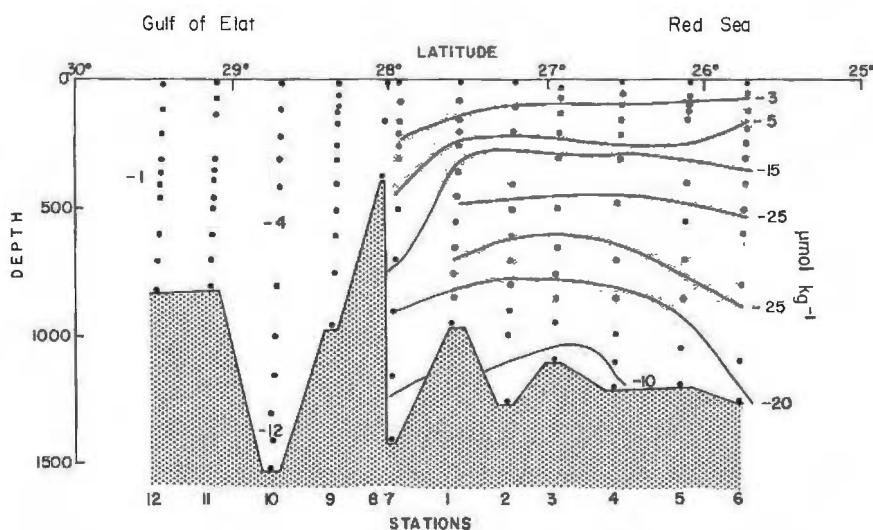


Figure 4  
 $\Delta\Sigma\text{CO}_2^0$  ( $\mu\text{mol kg}^{-1}$ ) cross-section in the Gulf of Elat and in the northern Red Sea. All  $\Delta\Sigma\text{CO}_2^0$  values have uncertainties  $\pm 10\ \mu\text{mol kg}^{-1}$ .

imentally during the GEOSECS cruise with a correction on  $-0.015 \text{ mmol kg}^{-1}$  as was recommended by Taro Takahashi on page 7 in Weiss *et al.* (1983). However, we would like to emphasize here that this correction is responsible only for the very negligible difference in  $\Delta\Sigma \text{CO}_2^0$  values (*ca.*  $0.06 \text{ } \mu\text{mol kg}^{-1}$ ) calculated with and without this correction. Even when we used the  $\Sigma \text{CO}_2$  values obtained by the same computing procedure as for our cruise, a similar depth profile of  $\Delta\Sigma \text{CO}_2^0$  for station 405 (GEOSECS) was obtained within the uncertainty stated above as  $\pm 10 \text{ } \mu\text{mol kg}^{-1}$ . As may be seen from Figure 3, the maximum negative  $\Delta\Sigma \text{CO}_2^0$  values for both the cruises are the same and situated at the same depth. The agreement between these two sets of data is excellent, showing that the excess  $\text{CO}_2$  values did not change over a period of four years, and perhaps longer, since there is no evidence that this signal did not exist much earlier than 1977.

Therefore, even though the excess anthropogenic  $\text{CO}_2$  signal reported in this article can be considered only as a qualitative one, owing to uncertainties in the calculations, it can be used as a valuable tracer for water mass formation and deep circulation in the northern Red Sea.

## REFERENCES

- Anati D. A. (1980). A parametrization of the geometry of sea straits. *Oceanologica Acta*, **3**, 395-397.
- Anderson L. and D. Dyrssen (1981). Chemical constituents of the Arctic Ocean in the Svalbard area. *Oceanologica Acta*, **4**, (3), 305-311.
- Anderson N. R. and A. Malahoff, editors (1977). *The fate of fossil fuel CO<sub>2</sub> in the oceans*. Plenum Press, 749 pp.
- Andrié C. and L. Merlivat (1989). Contribution of deuterium, oxygen-18, helium-3 and tritium isotopic data to the study of the Red Sea circulation. *Oceanologica Acta*, **12**, 3, 165-174.
- Ben-Avraham Z., Z. Garfunkel, G. Almagor and J. K. Hall (1979). Continental breakup by leaky transform: the Gulf of Elat (Aqaba). *Science*, **206**, 214-216.
- Bently C. R. (1983). The West Antarctic ice sheet: diagnosis and prognosis. *Proceedings of the Carbon Dioxide Research Conference, Berkeley Spring, W. Va.*, 1982, IV, 3-IV, 50.
- Boulaidd M. and J.-F. Minster (1989). Oxygen consumption and nutrient regeneration ratios along isopycnal horizons in the Pacific Ocean. *Mar. Chem.*, **26**, 133-153.
- Brewer P. G. (1978). Direct observation of the oceanic  $\text{CO}_2$  increase. *Geophys. Res. Letts.*, **5**, 997-1000.
- Broecker W. S. (1974). *Chemical oceanography*. Harcourt Brace Jovanovich, 22-26; 59-67.
- Broecker W. S. and T.-H. Peng (1982). *Tracers in the sea*. Lamont-Doherty Geological Observatory, New York.
- Broecker W. S., T. Takahashi, H. J. Simpson and T. H. Peng (1979). Fate of fossil fuel carbon dioxide and the global carbon budget. *Science*, **206**, 409-418.
- Cember R. P. (1988). On the sources, formation and circulation of Red Sea deep water. *J. geophys. Res.*, **93**, C7, 8175-8191.
- Chen C. T. (1980). Use of the anthropogenic  $\text{CO}_2$  signal as a tracer in the Southern Ocean. *Trans. Am. geophys. Un.*, **61**, 263.
- Chen C. T. (1982). On the distribution of anthropogenic  $\text{CO}_2$  in the Atlantic and Southern oceans. *Deep-Sea Res.*, **29**, 563-580.
- Chen C. T. and E. T. Drake (1986). Carbon dioxide increase in the atmosphere and oceans and possible effects on climate. *Ann. rev. Earth planet. Sci.*, **14**, 201-235.
- Chen C. T. and H. L. Lin (1987). Causes and effects of sea level rise. *J. environ. Protect. Soc. Rep. China*, **10**, 1-8.
- Chen C. T. and F. J. Millero (1979). Gradual increase of oceanic carbon dioxide. *Nature*, **277**, 205-206.
- Chen C. T. and R. M. Pytkowicz (1979). On the total  $\text{CO}_2$ -titration alkalinity-oxygen system in the Pacific Ocean. *Nature*, **281**, 362-365.
- Chen C. T., R. M. Pytkowicz and E. J. Olson (1982a). Evaluation of the calcium problem in the South Pacific. *Geochem. J.*, **16**, 1-10.
- Chen C. T., F. J. Millero and R. M. Pytkowicz (1982b). Comment on calculating the oceanic  $\text{CO}_2$  increase: a need for caution by A. M. Shiller. *J. geophys. Res.*, **87**, 2083-2085.
- Dyrssen D. and M. Wedborg (1982). The influences of the partial pressure of carbon dioxide on the total carbonate of seawater. *Mar. Chem.*, **11**, 183-185.
- Edmond J. M. (1970). High precision determination of titration alkalinity and total carbon dioxide content of sea water by potentiometric titration. *Deep-Sea Res.*, **17**, 737-750.
- Hoffman J. B., D. Keyes and J. G. Titus (1983). *Projecting future sea level rise-methodology, estimates to the year 2100, and research needs*. 2nd ed. Off. Policy Resour. Mgmt. Rep., EPA, Washington, D.C., 121 pp.
- Jones E. P. and E. M. Levy (1981). Oceanic  $\text{CO}_2$  increase in Baffin Bay. *J. mar. Res.*, **39**, 405-416.
- Kellogg W. W. (1979). Influences of mankind on climate. *Ann. rev. Earth planet. Sci.*, **7**, 63-92.
- Klinker J., Z. Reiss, C. Kropach, I. Levanon, H. Harpaz, E. Kalicz and G. Assaf (1976). Observations on the circulation pattern in the Gulf of Elat (Aqaba), Red Sea. *Israel J. Earth-Sci.*, **25**, 85-103.
- Kroopnick P. M. (1985). The distribution of  $^{13}\text{C}$  of  $\Sigma \text{CO}_2$  in the world oceans. *Deep-Sea Res.*, **32**, 57-84.
- Krumgalz B. S. and J. Erez (1984). Chemical oceanography survey of the northern Red Sea, the Straits of Tiran and the Gulf of Elat. *Israel Oceanogr. Limnol. Res., Haifa, Rep.*, **H3/84**, 133 pp.
- Kumar A. (1985). Distribution of pH in the central Arabian Sea by Redfield-Ketchum and Richard's model. *Curr. Sci.*, **54**, 1137-1138.
- Maillard C. (1974). Eaux intermédiaires et formation d'eau profonde en Mer Rouge. In: *L'Océanographie physique de la Mer Rouge, IAPSO-UNESCO-SCOR Symposium, Actes du Colloques, Vol. 2*, 105-130.
- Manins P. C. (1973). A filling box model of the deep circulation of the Red Sea. *Mém. Soc. R. Sci. Liège, Sér. 6*, **6**, 153-166.

## Acknowledgements

The authors thank many individuals and institutions for cooperation and support in connection with the *Tiran-02* expedition to the northern Red Sea and the Gulf of Elat in 1982. Our thanks are due to the Israel Ministry of Energy and Infrastructure, the Israel National Committee for Research and Development, and the National Science Council of the Republic of China for their financial support. B. S. K. and J. E. express special thanks to the captain and the crew of the R/V *Shikmona* and to the personnel of the Physical Oceanography Department of IOLR for their diligent efforts during the sample collection. Special appreciation is extended to two anonymous referees whose very valuable comments helped us to improve the presentation of our data. The authors thank Ms. K. Diskin for editing and typing the manuscript, Ms. E. Magdal for her help with the computer, and Ms. H. Bernard for drawing the draphs.

- Mehrbach C., C. H. Culberson, J. E. Hawley and R. M. Pytkowicz (1973). Measurement of the apparent dissociation constants of carbonic acid in seawater at atmospheric pressure. *Limnol. Oceanogr.*, **18**, 897-907.
- Mercer J. H. (1978). West Antarctic ice sheet and CO<sub>2</sub> greenhouse effect: a threat of disaster. *Nature*, **271**, 321-325.
- Metzl N., B. Moore, A. Papaud and A. Poisson (1989). Transport and carbon exchange in the Red Sea; inverse methodology. *Global biogeochem. Cycles*, **3**, 1-26.
- Millero F. J. (1979). The thermodynamics of the carbonate system in seawater. *Geochim. cosmochim. Acta*, **43**, 1651-1661.
- Millero F. J., J. W. Morse and C. T. Chen (1979). The carbonate system in the western Mediterranean sea. *Deep-Sea Res.*, **26**, 1395-1404.
- Minster J. F. and M. Boulahdid (1987). Redfield ratios along isopycnal surfaces - a complementary study. *Deep-Sea Res.*, **34**, 1981-2003.
- Moore B. III (1987). The oceanic sink for excess atmospheric carbon dioxide. In: *Wastes in the ocean*, vol. 4. I. W. Duedall, D. R. Kester, P. K. Park and B. H. Ketchum, editors, John Wiley and Sons, Ltd., 95-125.
- Morcos S. A. (1970). Physical and chemical oceanography of the Red Sea. *Oceanogr. mar. Biol. a. Rev.*, **8**, 73-202.
- Murray S. P., A. Hecht and A. Babcock (1984). On the mean flow in the Tiran Strait in winter. *J. mar. Res.*, **42**, 265-287.
- Naqvi S. W. A., H. P. Hansen and T. W. Kureishy (1986). Nutrient uptake and regeneration ratios in the Red Sea with reference to the nutrient budgets. *Oceanologica Acta*, **9**, 3, 271-275.
- Paldor N. and D. A. Anafi (1979). Seasonal variations of temperature and salinity in the Gulf of Elat (Aqaba). *Deep-Sea Res.*, **26**, 661-672.
- Papaud A. and A. Poisson (1986). Distribution of dissolved CO<sub>2</sub> in the Red Sea and correlations with other geochemical tracers. *J. mar. Res.*, **44**, 385-402.
- Peng T. H. and W. S. Broecker (1987). C/P ratios in marine detritus. *Global biogeochem. Cycles*, **1**, 155-161.
- Poisson A. and C. T. Chen (1987). Why is there little anthropogenic CO<sub>2</sub> in the Antarctic bottom water? *Deep-Sea Res.*, **34**, 1255-1275.
- Poisson A., S. Morcos, E. Souvermezoglou, A. Papaud and A. Ivanoff (1984). Some aspects of biogeochemical cycles in the Red Sea with special reference to new observations made in summer 1982. *Deep-Sea Res.*, **31A**, 707-718.
- Redfield A. C., B. H. Ketchum and F. A. Richards (1963). The influence of organisms on the composition of sea water. In: *The Sea, Ideas and Observations*, vol. 2, Intersciences, New York, 26-77.
- Revelle R. (1983). Probable future changes in sea-level resulting from increased atmospheric carbon dioxide. Nat. Res. Council., Comm. on Phys. Sci., Math. and Resour., 433-438.
- Ross D. A. (1983). The Red Sea. In: *Ecosystems of the world. 26: Estuaries and enclosed seas*. B. H. Ketchum, editor, Elsevier, 293-307.
- Shiller A. M. (1981). Calculating the oceanic CO<sub>2</sub> increase: a need for caution. *J. geophys. Res.*, **86**, 11083-11088.
- Southam J. R. and W. H. Peterson (1985). Transient response of the marine carbon cycle. In: *The carbon cycle and atmospheric CO<sub>2</sub>: natural variations archean to present*. E. T. Sundquist and W. S. Broecker, editors, Geophys. Monogr. 32. American Geophysical Union, Washington, D.C., 89-98.
- Strickland J. D. H. and T. R. Parsons (1972). A practical handbook of seawater analysis. *Bull. Fish. Res. Bd. Can.*, **167**.
- Stuiver M. (1978). Atmospheric carbon dioxide and carbon reservoir changes. *Science*, **199**, 253-258.
- Takahashi T., R. F. Weiss, C. H. Culberson, J. M. Edmond, D. E. Hammond, C. S. Wong, Y. H. Li and A. E. Bainbridge (1970). A carbonate chemistry profile at the 1969 GEOSECS intercalibration station in the eastern Pacific Ocean. *J. geophys. Res.*, **75**, 7648-7666.
- Takahashi T., W. S. Broecker and S. Langer (1985). Redfield ratio based on chemical data from isopycnal surfaces. *J. geophys. Res.*, **90**, 6907-6924.
- Thompson S. L. and S. H. Schneider (1981). Carbon dioxide and climate: ice and ocean. *Nature*, **290**, 9-10.
- UNESCO (1981). UNESCO/ICES/SCOR/IAPSO Joint Panel on Oceanographic Tables and Standards. Background papers and supporting data on the International Equation of State of Seawater 1980. *UNESCO tech. Pap. mar. Sci.*, **38**, 192 pp.
- UNESCO (1983). Chemical methods for use in marine environmental monitoring. *Manuals and Guides*, No. **12**, 5.
- Weiss R. F. (1970). The solubility of nitrogen, oxygen and argon in water and seawater. *Deep-Sea Res.*, **17**, 721-735.
- Weiss R. F., W. S. Broecker, H. Craig and D. Spencer (1983). *GEOSECS Indian Ocean Expedition*, vol. 5. Hydrographic Data, 1977-1978. National Science Foundation, Washington, D.C.